Thromboinflammation in high-risk human populations

Yuan, L.

CHAPTER 6

High-density lipoprotein composition related to endothelial dysfunction is associated with disease outcome in COVID-19 patients

Lushun Yuan[1,2], Aswin Verhoeven[3], Shuzhen Cheng[1,4], Wendy M.P.J. Sol[1], Ton J. Rabelink[1,2], Martin Giera[3,5], Bernard M. van den Berg[1,2,5], in collaboration with the BEAT-COVID study group[5]

[1] Einthoven Laboratory for Vascular and Regenerative Medicine, Leiden University Medical Center, Leiden, the Netherlands.

[2] Department of Internal Medicine, Division of Nephrology, Leiden University Medical Center, Leiden, the Netherlands.

[3] Center for Proteomics and Metabolomics, Leiden University Medical Center, Leiden, the Netherlands.

[4] Department of Internal Medicine, Division of Thrombosis and Hemostasis, Leiden University Medical Center, Leiden, the Netherlands.

[5]BEAT-COVID study group

Abstract

Background: Previous studies showed that endothelial dysfunction is involved in COVID-19 progression and high-density lipoproteins (HDL) have a variety of endothelial-protective properties. When considering that HDL composition is more representative of HDL function than HDL cholesterol (HDL-C) levels alone, we sought to investigate whether changes in HDL composition is associated with endothelial function and disease outcome in COVID-19 patients and lead to new risk stratification biomarkers.

Methods: Using ^{1}H nuclear magnetic resonance (NMR) spectroscopy and Bruker IVDr Lipoprotein Subclass Analysis (B.I.LISA^{TM}) software, an in-depth analysis of plasma lipoproteins was undertaken in a longitudinal study of COVID-19 patients with samples of healthy individuals as control.

Results: Higher triglyceride content in all HDL subclasses and lower HDL-4 plasma concentrations were found in COVID-19 patients compared to control, correlating with sequential organ failure assessment, circulating endothelial activation markers, and *in vitro* endothelial functional assay parameters.

Conclusion: The observed changes in HDL composition in COVID-19 patients which are associated with disease progression and possible survival suggest that these findings might be used as prognostic biomarkers in hospitalized COVID-19 patients.

Keywords: High-density lipoprotein composition, NMR, longitudinal, COVID-19, endothelial function

Introduction

The new coronavirus disease (COVID-19) caused by severe acute respiratory syndrome coronavirus-2 (SARS-CoV-2) led to a major worldwide pandemic characterized by acute lung injury and rapidly progressing to acute respiratory distress syndrome (ARDS) [1]. Previously, we showed that endothelial dysfunction, leading to endothelial glycocalyx degradation, barrier failure, and procoagulant surface formation was involved in COVID-19 progression [2]. In addition, early studies of lipid metabolism in patients revealed a role for high-density lipoproteins (HDL) protective factors in a variety of endothelial functions such as antioxidant, anti-inflammatory, anti-thrombotic, and even anti-infectious properties [3,4]. Recently, it was observed that the metabolic lipid profile in COVID-19 patients in the intensive care unit (ICU) was different when compared to healthy controls but also from patients with cardiogenic shock in ICU. [5]

Increasing evidence suggested that low serum HDL-cholesterol (HDL-C) levels at hospital admission is associated with disease severity and mortality in COVID-19 [6,7]. However, other studies revealed that the HDL lipidome and proteome rather than quantitative HDL-C concentration played a more representative role in HDL function during disease [8,9]. In addition to HDL-C concentrations in COVID-19, several studies showed significant inflammatory remodeling of the HDL proteome, associated with COVID-19 disease severity in both adult and pediatric COVID-19 patients [9-11].

However, limited studies are still available that show an association between COVID-19 related endothelial dysfunction and HDL composition and function. Furthermore, data is lacking whether the endothelial function related HDL composition is associated with disease outcome. Therefore, in the current study we used ^{1}H Nuclear magnetic resonance (NMR) spectroscopy and the validated Bruker IVDr Lipoprotein Subclass Analysis (B.I.LISA^{TM}) software [12-17] to measure blood HDL subclasses and lipid content concentrations in longitudinally collected serum samples from ICU and non-ICU, together with age-matched healthy controls. With the help of this in-depth analysis, we aimed to

identify changes in HDL composition in COVID-19 patients compared to healthy individuals and disease progression, screen for endothelial function related HDL composition, and investigate whether specific HDL compositional changes could lead to different outcomes in the course of the disease.

Material and methods

Study population.

A prospective observational cohort study was set up, in which patients with PCR-confirmed SARS-CoV-2 infection after hospital admission were recruited from April 2020 until August 2020, before the use of medication such as dexamethasone and vaccines were implemented. In the present study longitudinally collected plasma and serum samples from 37 patients with confirmed SARS-CoV-2 infection together with 12 age-matched controls were used (Figure 1A and supplemental figure S1). Patient characteristics are shown in supplemental table S1. Age-matched healthy donors with a male: female ratio of 2:1, were included after confirmed negative for SARS-CoV-2 IgG. The trial was registered in the Dutch Trial Registry (NL8589). Ethical approval was obtained from the Medical Ethical Committee Leiden-Den Haag-Delft (NL73740.058.20).

Sample preparation for ^{1}H nuclear magnetic resonance (NMR) spectroscopy.

Sample preparation was performed consistently with the requirements of the Bruker B.I.LISA lipoprotein analysis protocol. The EDTA plasma samples were thawed at room temperature and immediately homogenized by inverting the tubes 10 times. Next, 200µL of plasma was manually transferred to a Ritter 96 deep-well plate. A Gilson 215 liquid handler robot was used to mix 120µL of plasma with 120µL, 75 mM disodium phosphate buffer in H_2O/D_2O (80/20) with a pH of 7.4 containing 6.15 mM NaN_3 and 4.64 mM sodium

3-[trimethylsilyl] d4-propionate (Cambridge Isotope Laboratories). Using a modified second Gilson 215 liquid handler, 190µL of each sample was transferred into 3 mm Bruker SampleJet NMR tubes. Subsequently, the tubes were sealed by POM ball insertion and transferred to the SampleJet autosampler where they were kept at 6°C while queued for acquisition.

NMR spectroscopy measurement and processing.

All proton nuclear magnetic resonance (^{1}H-NMR) experiments were acquired on a 600 MHz Bruker Avance Neo spectrometer (Bruker Corporation, Billerica, USA) equipped with a 5-mm triple resonance inverse (TCI) cryogenic probe head with a Z-gradient system and automatic tuning and matching.

The NMR spectra were acquired following the Bruker B.I.Methods protocol. Before the measurements, a standard 3 mm sample of 99.8% methanol-d4 (Bruker) was used for temperature calibration [18]. A standard 3 mm QuantRefC sample (Bruker) was measured as the quantification reference and for quality control. All experiments were recorded at 310 K. The duration of the π/2 pulses was automatically calibrated for each sample using a homonuclear-gated nutation experiment on the locked and shimmed samples after automatic tuning and matching of the probe head [19]. For water suppression, presaturation of the water resonance with an effective field of γB1 = 25 Hz was applied during the relaxation delay and the mixing time of the NOESY1D experiment [20].

The NOESY1D experiment was recorded using the first increment of a NOESY pulse sequence with a relaxation delay of 4 s and a mixing time of 10 ms [21]. After applying 4 dummy scans, 32 scans of 98,304 points covering a sweep width of 17,857 Hz were recorded.

The lipoprotein values were extracted from the NOESY1D plasma spectra by submitting the data to the commercial Bruker IVDr Lipoprotein Subclass Analysis (B.I.LISA) platform [12-17].

This approach extracts information about lipoproteins and lipoprotein subfractions in plasma. In the current study, we focused on the HDL particles; dissected into concentration, composition, and four subclasses (sorted according to increasing density and decreasing size), and accompanying lipids within the lipoprotein subclasses including total cholesterol, free cholesterol, phospholipids, and triglycerides. The calculated esterified cholesterol was not included in the present study. Details about the measured HDL subfractions were listed in supplemental table S2.

HDL functional assay.

Primary human umbilical vein endothelial cells were isolated according to the previous protocol and cultured in 1% gelatin pre-coated flasks in endothelial growth medium (EGM2 medium, C-22011 supplemented with SupplementMix, Promocell, Heidelberg, Germany) with 1% antibiotics (penicillin/streptomycin, 15070063, Gibco, Paisley, UK). HDL isolation was isolated from 7 COVID-19 ICU individuals, pooled healthy control serum (pooled serum from 12 samples), and pooled non-ICU COVID-19 serum (pooled serum from 8 samples) based on the protocol from a previous study by Mulder *et al.* [22], stored on ice, and used the following day for HDL functionality tests. Primary human umbilical vein endothelial cells (HUVECs) were used to test HDL's anti-thrombotic properties. In the 96-well plate, HUVECs (passage 3) were seeded at a density of 4×10^5 cells/well. The following day, HUVECs were pre-incubated for 30 minutes with 2% apoB-depleted plasma or an equal volume of precipitation reagent in HEPES as a control. Tumor necrosis factor α (TNF-α, H8916, Sigma Aldrich, the Netherlands) was then added at a concentration of 10ng/mL. After another 5 hours of incubation, the cell surface was washed once with HBSS, no calcium, and no magnesium (14170120, Gibco™, Paisley, UK). Each well received 50µL of normal pooled plasma before being placed in the Fluorometer for a 10-minute incubation at 37°C. The formation of thrombin was started by mixing 10µL of the fluorogenic substrate with calcium (TS50.00 FluCa-kit; Thrombinoscope BV, Maastricht, the

Netherlands). The final reaction volume was 60µL. Thrombin formation was measured every 20 seconds for 60 minutes and calibrated using Thrombinoscope software (Additional file 1: Fig. S4a). To assess HDL anti-thrombotic capacity, we included all the parameters including thrombin peak height (Peak), endogenous thrombin potential (ETP), lag time, time to peak (ttPeak), and velocity of thrombin generation (VelIndex). To limit potential variation due to different plate conditions, HDL anti-thrombotic capacity measurements were performed at the same time using the same batch of pooled HUVECs and reagents. For each individual, measurements were taken in three technical replicates.

Statistical analyses.

Descriptive clinical and *in vitro* experimental characteristics of the study population were expressed as median with interquartile range (IQR) for non-normally distributed variables, mean with standard deviation (SD) for normally distributed variables, or percentages (%) for dichotomous variables. One-way ANOVA followed by Tukey's multiple comparisons test or Kruskal-Wallis followed by Dunn's multiple comparisons test were assessed for multiple groups. $P < 0.05$ were considered statistically significant.

Principle component analysis (PCA) was performed between healthy controls, non-ICU COVID-19 patients, and ICU COVID-19 patients based on HDL-related features.

Healthy control, non-ICU COVID-19, and ICU COVID-19 were considered as three outcomes, and concentrations of HDL-related features were scaled (z-normalization, i.e., with mean=0 and SD=1) to identify lipoproteins with different concentrations, and multinomial logistic regression analysis (MLR) was used. We set a specific reference for each comparison: between healthy control and non-ICU COVID-19, healthy control was the reference; between healthy control and ICU COVID-19, healthy control was the reference; between non-ICU COVID-19 and ICU COVID-19, non-ICU COVID-19 was the reference. We considered a p-value < 0.05 as significant. The results were expressed as a regression coefficient (β)

with a 95% confidence interval (CI) to evaluate the association between concentrations of HDL-related features and COVID-19.

Pearson's correlation analysis was performed between HDL-related features and clinical parameters, circulating markers (including soluble thrombomodulin, angiopoietin 2, and soluble syndecan-1), and *in vitro* endothelial functional assay parameters (including factor X activation, thrombin generation, endothelial barrier function, and supernatant endothelial activation markers) from our previously published paper [2].

We next stratified ICU COVID-19 patients into survivors and non-survivors and investigated HDL composition changes during disease development. The trend line for the longitudinal changes in HDL composition was performed according to loess regression. Additionally, we compared the changes in HDL subclasses between the first collected sample and the last sample during hospitalization. Statistical analyses were performed in R (version 4.1.0) and GraphPad Prism version 8 (Graphpad Inc., La Jolla, CA, USA).

Results

Clinical characteristics and experimental characteristics of the study population .

Supplemental table S1 shows the clinical and experimental characteristics of individuals in the present study. Of 37 included COVID-19 patients, 18.92% were women, with a median age of 61 years (interquartile range, 57–70 years). Among 37 COVID-19 patients, there were 5 non-ICU COVID-19 patients and 32 ICU COVID-19 patients (26 survivors and 6 non-survivors). Compared to non-ICU COVID-19 patients and healthy individuals, both ICU COVID-19 survivors and non-survivors had higher endothelial activation, higher disease severity, and higher *in vitro* serum induced endothelial activation. Notably, although not significant, ICU non-survivors revealed a more profound endothelial dysfunction phenotype than ICU survivors.

HDL anti-thrombotic capacity reduction in ICU COVID-19 patients.

The effect of purified HDL serum fractions of healthy individuals (n = 12, pooled), non-ICU COVID-19 patients (n = 5, pooled) and 7 survivor COVID-19 individuals in ICU was tested for its anti-thrombotic capacity on cultured endothelial cells. Based on the thrombin generation curve, the curves of most ICU COVID-19 patients were higher than the healthy control and non-ICU COVID-19 patient curves (supplemental Fig. S2A). Furthermore, the thrombin peak height, endogenous thrombin potential (ETP), and VelIndex were all higher in the ICU COVID-19 patients tested; whereas lag time and ttPeak were lower in ICU COVID-19 patients tested (supplemental Fig. S2B-F). These results that HDL functionality in anti-thrombin formation already could be impaired in COVID-19 patients when admitted to the ICU.

HDL composition in plasma can differentiate patients with COVID-19 from healthy controls.

PCA analysis on HDL-related features of all the samples (including controls, non-ICU and ICU patients), using the "ggfortify" R package revealed good separation of COVID-19 patients from healthy individuals (Fig. 1B). Further hierarchical clustering revealed that this division in HDL composition presented that triglyceride content in all HDL subclasses was standing out as a cluster with an increasing trend with disease severity (Fig. 1C).

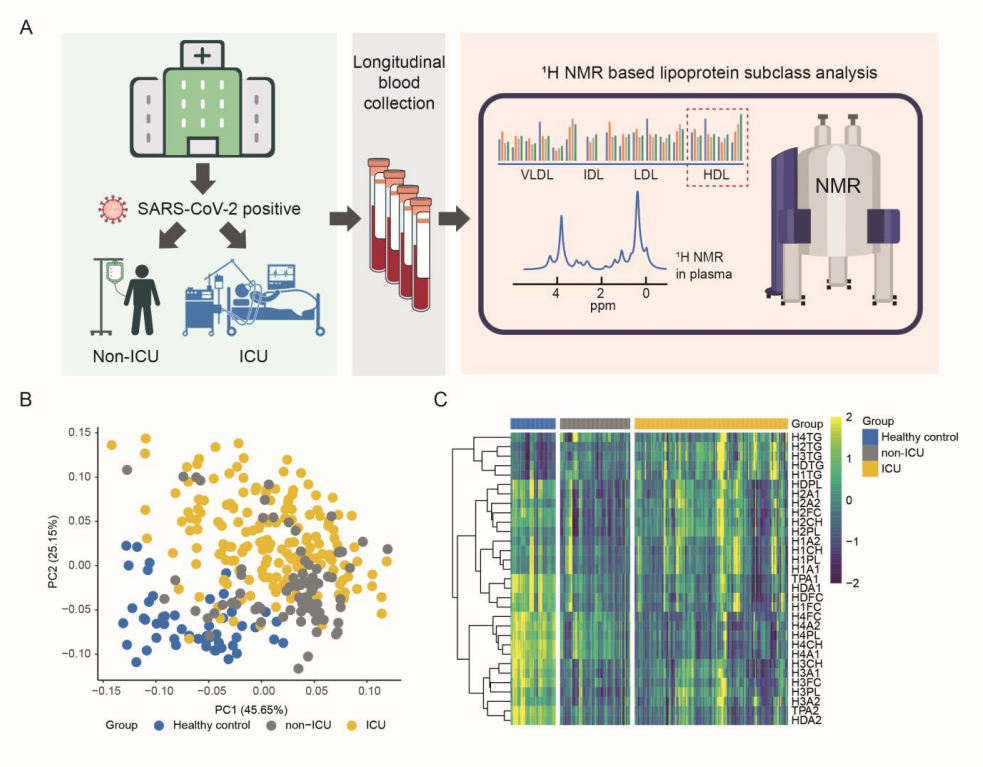

Figure 1. HDL composition between healthy individuals and COVID-19 patients based on ^{1}H NMR. (A) Scheme of study design and ^{1}H NMR in the present study. (B) Principal component analysis using HDL composition for longitudinally collected serum samples from ICU COVID-19 patients (yellow), non-ICU COVID-19 patients (grey), and samples from healthy controls (blue). (C) Heatmap showing overview of HDL composition in the present study indicating that triglyceride content in HDL subclasses increased with the disease progression whereas the rest of HDL composition such as HDL-4 subfractions decreased with the disease progression.

Distinct HDL composition between healthy controls, non-ICU COVID-19 patients, and ICU COVID-19 patients.

To identify further differences in HDL composition between the three groups multinomial logistic regression analysis was used. This analysis revealed that all HDL compositions (27

lower and 5 higher) were significantly different between healthy controls and non-ICU COVID-19 patients (Fig 2A, B and supplemental table S3) while 27 HDL subfractions (22 lower and 5 higher) differed significantly between healthy controls and ICU COVID-19 patients (Fig 2C, D and supplemental table S4). Comparing non-ICU and ICU COVID-19 patients showed notable changes in all the small and dense HDL subfractions which were lower in ICU COVID-19 patients and with a much higher triglyceride content in most HDL subclasses (Fig 2E, F and supplemental table S5). In addition, between COVID19 patients in ICU and not in ICU the HDL1-3 subfractions were significantly increased (Fig 2E, F and supplemental table S5).

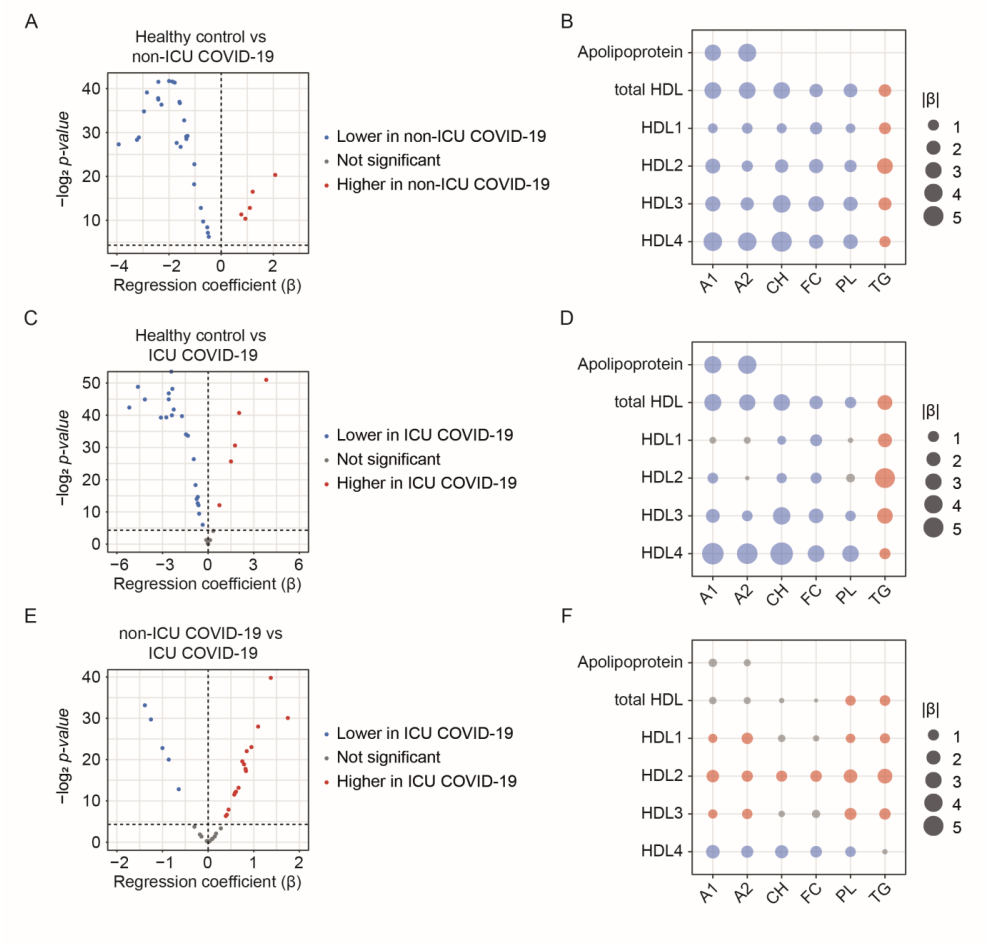

Figure 2. Differential HDL composition between ICU COVID-19, non-ICU COVID-19 patients, and healthy individuals. (A) Volcano plot and (B) Bubble plot of differential lipoprotein subfractions between non-ICU COVID-19 patients and healthy controls. (C) Volcano plot and (D) Bubble plot of differential lipoprotein subfractions between ICU COVID-19 patients and healthy controls. (E) Volcano plot and (F) Bubble plot of differential lipoprotein subfractions between ICU COVID-19 patients and non-ICU COVID-19 patients. Dot size of the bubble plot represented the absolute value of effect size based on MLR. The red color represented a higher concentration in the reference group, while the blue color represented a lower concentration in the reference group.

Associations between HDL composition and clinical and experimental parameters.

We next investigated the associations between HDL composition and clinical and experimental parameters (i.e, circulating markers, clinical assessment parameters, and *in vitro* endothelial functional assay parameters) using Pearson's correlation analysis. A positive correlation was observed between HDL-1-3 subclass triglyceride content and circulating endothelial activation markers angiopoietin 2, sequential organ failure assessment (SOFA) score, LUMC severity score, and respiratory failure assessment (Fig 3). These observations were also observed with the *in vitro* endothelial coagulation data from the Xa and thrombin generation measurements, endothelial activation markers in the supernatant, and endothelial barrier function loss. The HDL-4 subfraction only showed negative correlations with circulating and *in vitro* endothelial activation parameters. Furthermore, apolipoprotein A1 (ApoA1), total cholesterol, and free cholesterol content in each of the HDL subclasses were found to be negatively associated with endothelial activation and disease severity.

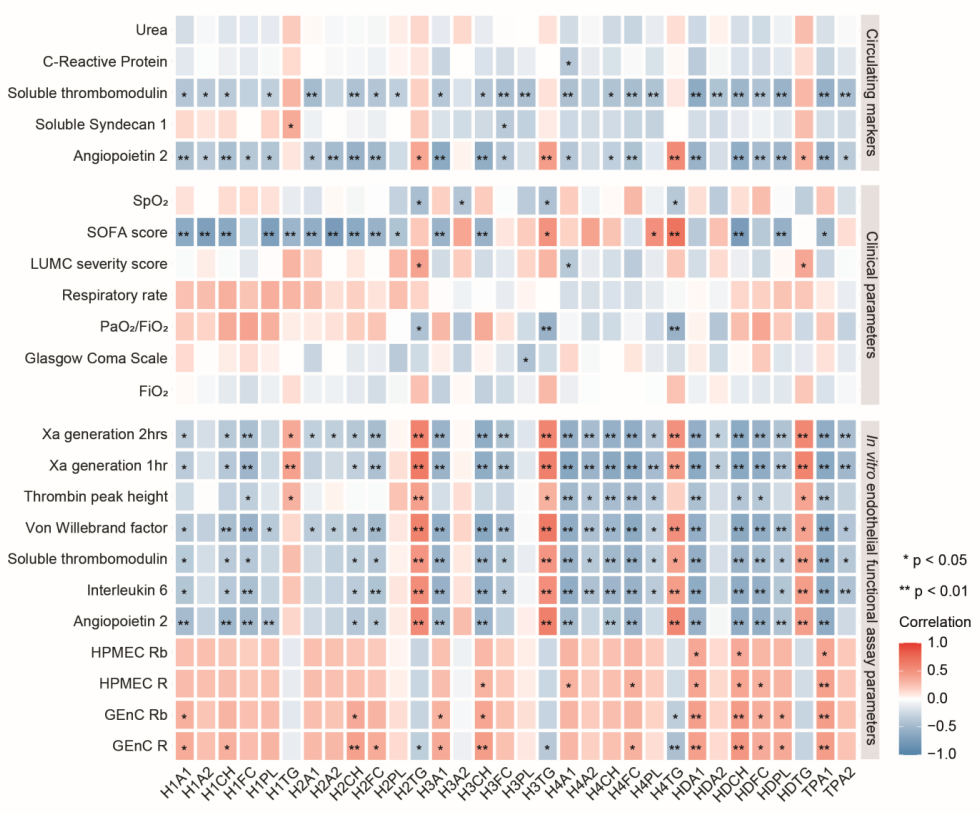

Figure 3. Correlation heatmap of circulating markers, clinical parameters, in vitro endothelial functional assay parameters, and HDL composition. The red indicated a positive correlation, while the blue indicated a negative correlation. Shading color and asterisks represented the value of corresponding correlation coefficients (*p < 0.05; **p < 0.01).

Triglyceride content in HDL subclasses showed distinct longitudinal changes between non-ICU COVID-19 patients, ICU COVID-19 survivors, and ICU COVID-19 non-survivors.

Since triglyceride content in all the HDL subclasses was increased in COVID-19 patients compared to healthy individuals and associated with disease severity and clinical parameters, we then made the stratification analysis and evaluated the changes in disease

course. We found that most of the triglyceride content in HDL subclasses except in HDL-4, was initially higher in ICU non-survivors than in ICU survivors and non-ICU patients, and when it reached the peak (almost twice the levels of healthy individuals) and remained higher over time than in ICU survivors and non-ICU patients until the patients died (Fig 4A, C, E, G, I). Compared to the first collected sample in ICU with the last collected sample during hospitalization, only HDTG, H1TG, and H4TG were higher in the last collected samples than in the first collected samples in the ICU non-survivor group; H2TG and H3TG remained or decreased a bit. It is worth noting that all HDL subclass triglyceride was much higher in ICU non-survivors than in ICU survivors and non-ICU patients (Fig 4B, D, F, H, J).

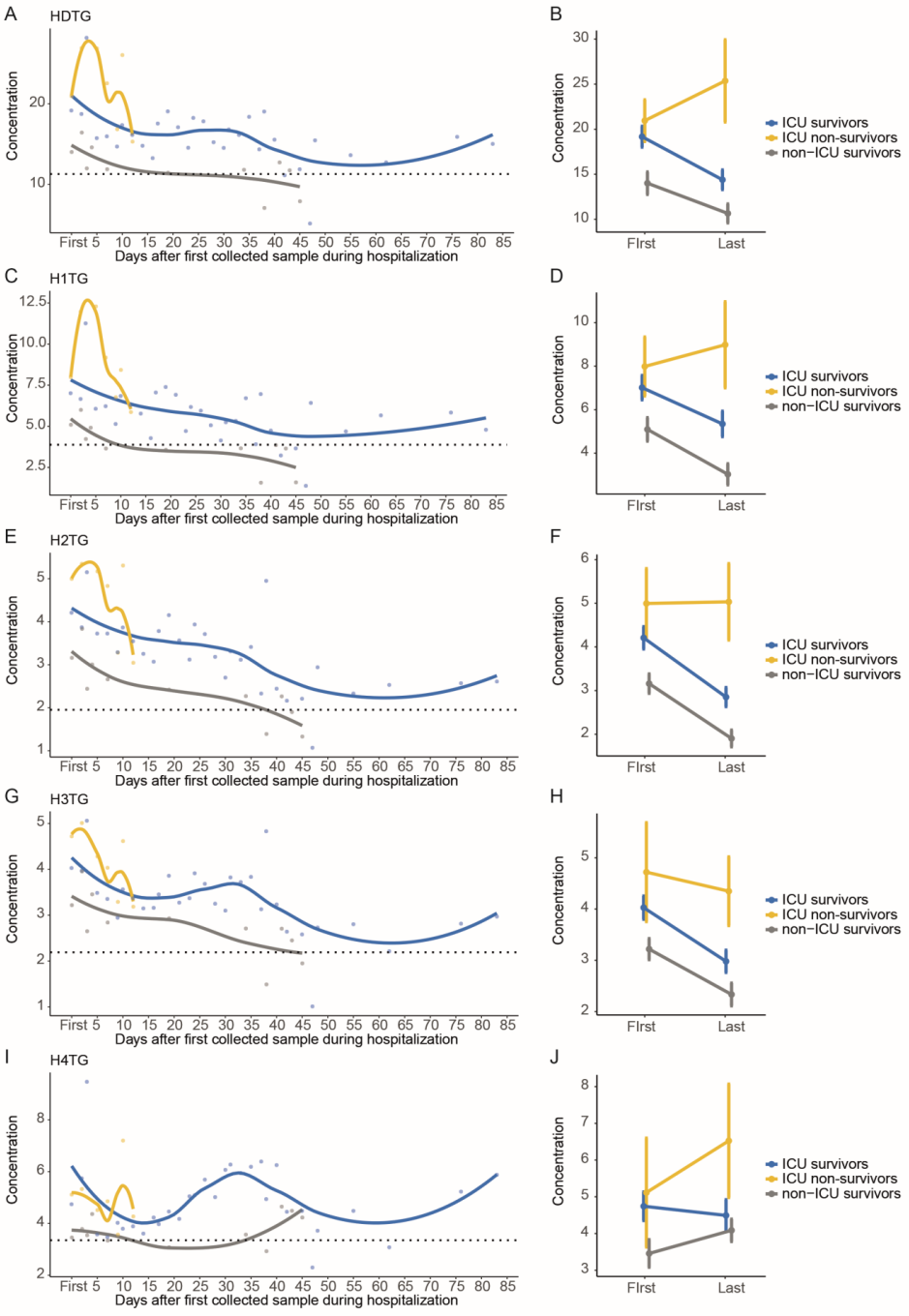
A
HDTG
Concentration
Days after first collected sample during hospitalization
B
C
H1TG
D
E
H2TG
F
G
H3TG
H
I
H4TG
J
ICU survivors
ICU non-survivors
non−ICU survivors
First
Last

Figure 4. Changes of triglyceride content in HDL subclasses in the course of the disease of ICU survivors, non-survivors, and non-ICU patients. (A) HDTG changes during hospitalization. (B) HDTG changes between the first and last collected samples during hospitalization. (C) H1TG changes during hospitalization. (D) H1TG changes between the first and last collected samples during hospitalization. (E) H2TG changes during hospitalization. (F) H2TG changes between the first and last collected samples during hospitalization. (G) H3TG changes during hospitalization. (H) H3TG changes between the first and last collected samples during hospitalization. (I) H4TG changes during hospitalization. (J) H4TG changes between the first and last collected samples during hospitalization. The dashed line represented the average concentration of triglyceride content in HDL subclasses in healthy individuals.

HDL-4 subfraction showed distinct longitudinal changes between non-ICU COVID-19 patients, ICU COVID-19 survivors, and ICU COVID-19 non-survivors.

The HDL-4 subfraction was lower in ICU COVID-19 patients than in non-ICU COVID-19 patients. Investigating HDL-4 subfraction changes during the disease progression revealed that both concentrations continuously increased over time in non-ICU and ICU survivors (Fig 5). In ICU non-survivors, the levels first decreased then increased a little bit which were much lower than those in healthy individuals, especially H4A1. We also noticed that although the concentrations of HDL-4 subfractions increased in non-ICU and ICU survivors, they were still much lower than in healthy individuals (Fig 5A, C, E, G, I). We did not find any difference in HDL-4 subfractions at the initial time point, but we discovered that there were notable differences between the three groups in the last collected samples regarding the highest concentrations of HDL-4 subfractions in non-ICU and lowest concentrations of HDL-4 subfractions in ICU non-survivors (Fig 5B, D, F, H, J).

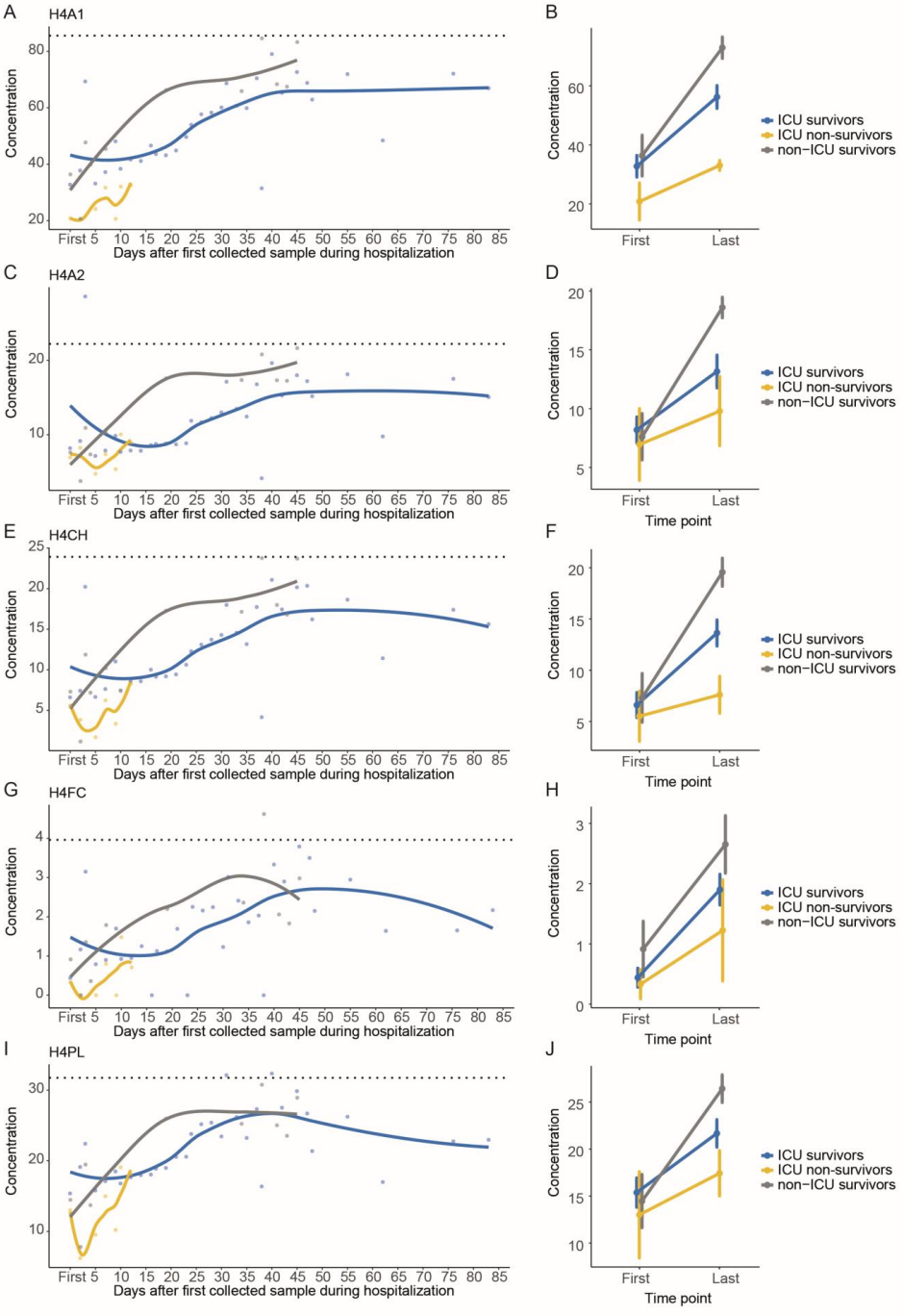
A
H4A1
Concentration
Days after first collected sample during hospitalization
B
C
H4A2
D
E
H4CH
F
G
H4FC
H
I
H4PL
J
First
Last
Time point
ICU survivors
ICU non-survivors
non−ICU survivors

Figure 5 Changes of HDL-4 subfractions in the course of the disease of ICU survivors, non-survivors, and non-ICU patients. (A) H4A1 changes during hospitalization. (B) H4A1 changes between the first and last collected samples during hospitalization. (C) H4A2 changes during hospitalization. (D) H4A2 changes between the first and last collected samples during hospitalization. (E) H4CH changes during hospitalization. (F) H4CH changes between the first and last collected samples during hospitalization. (G) H4FC changes during hospitalization. (H) H4FC changes between the first and last collected samples during hospitalization. (I) H4PL changes during hospitalization. (J) H4PL changes between the first and last collected samples during hospitalization. The dashed line represented the average concentration of HDL-4 subfractions in healthy individuals.

Discussion

In the current study, we found that increased levels of triglycerides in all HDL subclasses and decreased levels of HDL-4 subfractions with disease progression. Altered HDL composition was correlated with SOFA score, circulating endothelial activation markers, and *in vitro* endothelial functional assay parameters, and was associated with distinct disease outcomes. Our findings indicate that changes in HDL composition might be used for risk stratification in disease progression in COVID-19 patients.

In general, higher triglyceride content in most of the HDL subclasses and HDL-4 subfractions were found in COVID-19 patients. These HDL compositional changes that we observed for COVID-19 compared with healthy individuals were in line with previous studies in Germany, Spain, and Australia [5,23,24]. This finding further confirmed previous studies and proved that the NMR-based lipoprotein profiling technique was quite robust and may be clinically meaningful beyond the routine clinical chemistry measurement.

Our study, for the first time, linked the HDL composition with the *in vitro* endothelial functional assay parameters and identified the specific endothelial function related to HDL composition. Accumulating evidence suggested that hypertriglyceridemia was an independent risk factor for endothelial dysfunction [25]. We observed that triglyceride content in HDL subclasses was positively correlated with circulating endothelial activation marker Angiopoietin 2 which was relevant in respiratory and thrombotic related disorders in COVID-19 ICU patients, showing unfavorable prognostic value [26]. Syndecan 1, one of the endothelial glycocalyx core proteins, was reported as a marker for disease progression and severity classification of COVID-19 [27-29]. Also, we discovered that triglyceride content in HDL-1 showed a positive correlation with soluble Syndecan 1, implying that triglyceride content in large HDL may lead to more aggressive endothelial activation. Moreover, a comparison between non-ICU and ICU COVID-19 patients and the longitudinal changes concerning triglyceride content in HDL subclasses showed clear differences between non-ICU and ICU as well as ICU survivors and non-survivors, further supporting this concept.

Small and dense HDL particles are essential for cellular cholesterol efflux, antioxidative, antithrombotic, anti-inflammatory, and antiapoptotic functions [30,31]. Interestingly, our findings revealed that HDL-4 subfractions were lower in COVID-19 patients (both non-ICU and ICU) compared to healthy individuals. Moreover, COVID-19 patients in ICU even showed much lower concentrations of HDL-4 subfractions. Given that HDL-4 subfractions were negatively correlated with endothelial dysfunction, we hypothesized that a lack of specific vasoprotective HDL compositions would lead to disease progression, which was supported by the longitudinal changes in HDL-4 subfractions in COVID-19 patients with different outcomes.

Either higher triglyceride content in HDL subclasses or lower HDL-4 subfractions would cause dysfunction of HDL (data unpublished). The ICU non-survivors showed lower levels of HDL-4 subfractions and higher triglyceride content in HDL subclasses over time, which to some extent, implied that impaired HDL function with less vasoprotective functions might contribute to the worse outcome. Here, our in-house pilot HDL functional assay demonstrated that COVID-19 patients had impaired HDL function in terms of its capacity to suppress TNFα-induced procoagulant cell surface in endothelial cells which is also consistent with earlier findings that HDL from COVID-19 patients was less protective in endothelial cells stimulated by TNFα (permeability, VE-cadherin disorganization, and apoptosis) [32]. Following these findings, we discovered that COVID-19 patients showed greater changes in HDL composition, particularly triglyceride content in HDL subclasses and HDL-4 subfractions, which contributed to risk stratification for COVID-19.

The strength of our study is that we measured detailed HDL compositions in a longitudinal population with different disease severity and our study was the first to link HDL compositional changes with serum-induced endothelial functional assay parameters. Our findings further confirmed altered HDL composition in COVID-19 patients with regard to reduced HDL anti-thrombotic capacity, linking it with disease severity assessment and endothelial activation markers; meanwhile, we revealed disease outcome related HDL compositional changes. However, the present study has some limitations mainly related to

the relatively small sample size of the cohort, which might limit generalizability and eliminate the possibility of stratification analyses. In addition, we did not include any ICU patients without COVID-19 to compare whether our findings were general changes for patients ending up in ICU or disease specific changes. Besides, medication use such as lipid lowering medications could affect HDL concentration, composition, and function [33,34], which indicated that the changes in HDL composition were not solely affected by the disease. Another limitation is that we only performed a pilot in-house HDL functional assay, which, while promising, was insufficiently conclusive, and more experiments with more time points and patients were required.

Conclusions

To conclude, compared to healthy individuals, non-ICU and ICU COVID-19 patients had altered HDL composition, and lower HDL-4 subfractions and higher triglyceride content in HDL subclasses were associated with endothelial function and disease progression, which might be useful for risk stratification for patients with COVID-19 in ICU.

Abbreviations

ARDS: acute respiratory distress syndrome; B.I.LISATM: Bruker IVDr Lipoprotein Subclass Analysis; CI: confidence interval; SARS-CoV-2: coronavirus causing severe acute respiratory syndrome; ETP: endogenous thrombin potential; HDL: High-density lipoprotein; HDL-C: HDL-cholesterol; HUVEC: Human umbilical vein endothelial cell; ICU: intensive care unit; IQR: interquartile range; NMR: nuclear magnetic resonance; PCA: Principle component analysis; SOFA: sequential organ failure assessment; SD: standard deviation; Peak: thrombin peak height; ttPeak: time to peak; TNF-α: Tumor necrosis factor α; VelIndex: velocity of thrombin generation.

Acknowledgments

We thank all the patients and healthy volunteers who participated in this study. We express our gratitude to the researchers, nurses, and physicians who assisted in the organization of this study.

Authors' contributions

LY, MAG, and BMvdB contributed to the study concept, design, and analysis; LY analysed and interpreted data, and critically revised the manuscript; AV performed NMR measurements; LY, SZ, and WMPJS performed the *in vitro* endothelial functional assays; and LY, TJR, and BMvdB drafted the manuscript. The final manuscript was read, commented on, and approved by all authors.

Funding

This work was supported by the China Scholarship Council grant to Lushun Yuan (CSC no. 201806270262) and BEAT-COVID funding by Leiden University Medical Center.

Availability of data and materials

All data and methods supporting the findings of this study are available from the corresponding author upon reasonable request.

Ethics approval and consent to participate

The samples were from a trial registered in Dutch Trial Registry (NL8589). The study protocol was approved by the Institutional Review Board (Leiden University Medical Center, Leiden, The Netherlands), and ethical approval was obtained from the Medical Ethical Committee Leiden-Den Haag-Delft (NL73740.058.20).

Consent for publication

The manuscript was approved by all authors for publication.

Competing interests

The authors declare that they have no competing interests.

References

1. Chidambaram, V., Kumar, A., Majella, M.G., Seth, B., Sivakumar, R.K., Voruganti, D., Bavineni, M., Baghal, A., Gates, K., Kumari, A., et al. (2022). HDL cholesterol levels and susceptibility to COVID-19. EBioMedicine *82*, 104166. 10.1016/j.ebiom.2022.104166.

2. Yuan, L., Cheng, S., Sol, W., van der Velden, A.I.M., Vink, H., Rabelink, T.J., and van den Berg, B.M. (2022). Heparan sulfate mimetic fucoidan restores the endothelial glycocalyx and protects against dysfunction induced by serum of COVID-19 patients in the intensive care unit. ERJ Open Res *8*. 10.1183/23120541.00652-2021.

3. Tanaka, S., Couret, D., Tran-Dinh, A., Duranteau, J., Montravers, P., Schwendeman, A., and Meilhac, O. (2020). High-density lipoproteins during sepsis: from bench to bedside. Crit Care *24*, 134. 10.1186/s13054-020-02860-3.

4. Tran-Dinh, A., Diallo, D., Delbosc, S., Varela-Perez, L.M., Dang, Q.B., Lapergue, B., Burillo, E., Michel, J.B., Levoye, A., Martin-Ventura, J.L., and Meilhac, O. (2013). HDL and endothelial protection. Br J Pharmacol *169*, 493-511. 10.1111/bph.12174.

5. Schmelter, F., Foh, B., Mallagaray, A., Rahmoller, J., Ehlers, M., Lehrian, S., von Kopylow, V., Kunsting, I., Lixenfeld, A.S., Martin, E., et al. (2021). Metabolic and Lipidomic Markers Differentiate COVID-19 From Non-Hospitalized and Other Intensive Care Patients. Front Mol Biosci *8*, 737039. 10.3389/fmolb.2021.737039.

6. Mahat, R.K., Rathore, V., Singh, N., Singh, N., Singh, S.K., Shah, R.K., and Garg, C. (2021). Lipid profile as an indicator of COVID-19 severity: A systematic review and meta-analysis. Clin Nutr ESPEN *45*, 91-101. 10.1016/j.clnesp.2021.07.023.

7. Chidambaram, V., Shanmugavel Geetha, H., Kumar, A., Majella, M.G., Sivakumar, R.K., Voruganti, D., Mehta, J.L., and Karakousis, P.C. (2022). Association of Lipid Levels With COVID-19 Infection, Disease Severity and Mortality: A Systematic

Review and Meta-Analysis. Front Cardiovasc Med *9*, 862999. 10.3389/fcvm.2022.862999.

8. Jia, C., Anderson, J.L.C., Gruppen, E.G., Lei, Y., Bakker, S.J.L., Dullaart, R.P.F., and Tietge, U.J.F. (2021). High-Density Lipoprotein Anti-Inflammatory Capacity and Incident Cardiovascular Events. Circulation *143*, 1935-1945. 10.1161/CIRCULATIONAHA.120.050808.

9. Souza Junior, D.R., Silva, A.R.M., Rosa-Fernandes, L., Reis, L.R., Alexandria, G., Bhosale, S.D., Ghilardi, F.R., Dalcoquio, T.F., Bertolin, A.J., Nicolau, J.C., et al. (2021). HDL proteome remodeling associates with COVID-19 severity. J Clin Lipidol *15*, 796-804. 10.1016/j.jacl.2021.10.005.

10. Stadler, J.T., Mangge, H., Rani, A., Curcic, P., Herrmann, M., Pruller, F., and Marsche, G. (2022). Low HDL Cholesterol Efflux Capacity Indicates a Fatal Course of COVID-19. Antioxidants (Basel) *11*. 10.3390/antiox11101858.

11. Mietus-Snyder, M., Suslovic, W., Delaney, M., Playford, M.P., Ballout, R.A., Barber, J.R., Otvos, J.D., DeBiasi, R.L., Mehta, N.N., and Remaley, A.T. (2022). Changes in HDL cholesterol, particles, and function associate with pediatric COVID-19 severity. Front Cardiovasc Med *9*, 1033660. 10.3389/fcvm.2022.1033660.

12. Lounila, J., Ala-Korpela, M., Jokisaari, J., Savolainen, M.J., and Kesaniemi, Y.A. (1994). Effects of orientational order and particle size on the NMR line positions of lipoproteins. Phys Rev Lett *72*, 4049-4052. 10.1103/PhysRevLett.72.4049.

13. Jeyarajah, E.J., Cromwell, W.C., and Otvos, J.D. (2006). Lipoprotein particle analysis by nuclear magnetic resonance spectroscopy. Clin Lab Med *26*, 847-870. 10.1016/j.cll.2006.07.006.

14. Jiang, H., Peng, J., Zhou, Z.Y., Duan, Y., Chen, W., Cai, B., Yang, H., and Zhang, W. (2010). Establishing (1)H nuclear magnetic resonance based metabonomics fingerprinting profile for spinal cord injury: a pilot study. Chin Med J (Engl) *123*, 2315-2319.

15. Straat, M.E., Martinez-Tellez, B., Nahon, K.J., Janssen, L.G.M., Verhoeven, A., van der Zee, L., Mulder, M.T., Kooijman, S., Boon, M.R., van Lennep, J.E.R., et al. (2022). Comprehensive (apo)lipoprotein profiling in patients with genetic hypertriglyceridemia using LC-MS and NMR spectroscopy. J Clin Lipidol *16*, 472-482. 10.1016/j.jacl.2022.04.004.

16. Bakker, L.E., Boon, M.R., Annema, W., Dikkers, A., van Eyk, H.J., Verhoeven, A., Mayboroda, O.A., Jukema, J.W., Havekes, L.M., Meinders, A.E., et al. (2016). HDL functionality in South Asians as compared to white Caucasians. Nutrition, metabolism, and cardiovascular diseases : NMCD *26*, 697-705. 10.1016/j.numecd.2016.02.010.

17. Nodeland, M., Klevjer, M., Saether, J., Giskeodegard, G., Bathen, T.F., Wisloff, U., and Bye, A. (2022). Atherogenic lipidomics profile in healthy individuals with low cardiorespiratory fitness: The HUNT3 fitness study. Atherosclerosis *343*, 51-57. 10.1016/j.atherosclerosis.2022.01.001.

18. Findeisen, M., Brand, T., and Berger, S. (2007). A 1H-NMR thermometer suitable for cryoprobes. Magn Reson Chem *45*, 175-178. 10.1002/mrc.1941.

19. Wu, P.S., and Otting, G. (2005). Rapid pulse length determination in high-resolution NMR. J Magn Reson *176*, 115-119. 10.1016/j.jmr.2005.05.018.

20. Price, W.S. (1999). Water signal suppression in NMR spectroscopy. Annu Rep Nmr Spectro *38*, 289-354. Doi 10.1016/S0066-4103(08)60040-X.

21. Kumar, A., Ernst, R.R., and Wuthrich, K. (1980). A two-dimensional nuclear Overhauser enhancement (2D NOE) experiment for the elucidation of complete proton-proton cross-relaxation networks in biological macromolecules. Biochem Biophys Res Commun *95*, 1-6. 10.1016/0006-291x(80)90695-6.

22. Mulder, D.J., de Boer, J.F., Graaff, R., de Vries, R., Annema, W., Lefrandt, J.D., Smit, A.J., Tietge, U.J., and Dullaart, R.P. (2011). Skin autofluorescence is inversely related to HDL anti-oxidative capacity in type 2 diabetes mellitus. Atherosclerosis *218*, 102-106. 10.1016/j.atherosclerosis.2011.05.011.

23. Kimhofer, T., Lodge, S., Whiley, L., Gray, N., Loo, R.L., Lawler, N.G., Nitschke, P., Bong, S.H., Morrison, D.L., Begum, S., et al. (2020). Integrative Modeling of Quantitative Plasma Lipoprotein, Metabolic, and Amino Acid Data Reveals a Multiorgan Pathological Signature of SARS-CoV-2 Infection. Journal of proteome research *19*, 4442-4454. 10.1021/acs.jproteome.0c00519.

24. Bruzzone, C., Bizkarguenaga, M., Gil-Redondo, R., Diercks, T., Arana, E., Garcia de Vicuna, A., Seco, M., Bosch, A., Palazon, A., San Juan, I., et al. (2020). SARS-CoV-2 Infection Dysregulates the Metabolomic and Lipidomic Profiles of Serum. iScience *23*, 101645. 10.1016/j.isci.2020.101645.

25. Kajikawa, M., and Higashi, Y. (2019). Triglycerides and endothelial function: molecular biology to clinical perspective. Curr Opin Lipidol *30*, 364-369. 10.1097/MOL.0000000000000630.

26. Smadja, D.M., Guerin, C.L., Chocron, R., Yatim, N., Boussier, J., Gendron, N., Khider, L., Hadjadj, J., Goudot, G., Debuc, B., et al. (2020). Angiopoietin-2 as a marker of endothelial activation is a good predictor factor for intensive care unit admission of COVID-19 patients. Angiogenesis *23*, 611-620. 10.1007/s10456-020-09730-0.

27. Zhang, D., Li, L., Chen, Y., Ma, J., Yang, Y., Aodeng, S., Cui, Q., Wen, K., Xiao, M., Xie, J., et al. (2021). Syndecan-1, an indicator of endothelial glycocalyx

degradation, predicts outcome of patients admitted to an ICU with COVID-19. Mol Med *27*, 151. 10.1186/s10020-021-00412-1.

28. Suzuki, K., Okada, H., Tomita, H., Sumi, K., Kakino, Y., Yasuda, R., Kitagawa, Y., Fukuta, T., Miyake, T., Yoshida, S., et al. (2021). Possible involvement of Syndecan-1 in the state of COVID-19 related to endothelial injury. Thromb J *19*, 5. 10.1186/s12959-021-00258-x.

29. Ogawa, F., Oi, Y., Nakajima, K., Matsumura, R., Nakagawa, T., Miyagawa, T., Sakai, K., Saji, R., Taniguchi, H., Takahashi, K., et al. (2021). Temporal change in Syndecan-1 as a therapeutic target and a biomarker for the severity classification of COVID-19. Thromb J *19*, 55. 10.1186/s12959-021-00308-4.

30. Camont, L., Lhomme, M., Rached, F., Le Goff, W., Negre-Salvayre, A., Salvayre, R., Calzada, C., Lagarde, M., Chapman, M.J., and Kontush, A. (2013). Small, dense high-density lipoprotein-3 particles are enriched in negatively charged phospholipids: relevance to cellular cholesterol efflux, antioxidative, antithrombotic, anti-inflammatory, and antiapoptotic functionalities. Arteriosclerosis, thrombosis, and vascular biology *33*, 2715-2723. 10.1161/ATVBAHA.113.301468.

31. He, Y., Ronsein, G.E., Tang, C., Jarvik, G.P., Davidson, W.S., Kothari, V., Song, H.D., Segrest, J.P., Bornfeldt, K.E., and Heinecke, J.W. (2020). Diabetes Impairs Cellular Cholesterol Efflux From ABCA1 to Small HDL Particles. Circ Res *127*, 1198-1210. 10.1161/CIRCRESAHA.120.317178.

32. Begue, F., Tanaka, S., Mouktadi, Z., Rondeau, P., Veeren, B., Diotel, N., Tran-Dinh, A., Robert, T., Velia, E., Mavingui, P., et al. (2021). Altered high-density lipoprotein composition and functions during severe COVID-19. Sci Rep *11*, 2291. 10.1038/s41598-021-81638-1.

33. Orsoni, A., Therond, P., Tan, R., Giral, P., Robillard, P., Kontush, A., Meikle, P.J., and Chapman, M.J. (2016). Statin action enriches HDL3 in polyunsaturated phospholipids and plasmalogens and reduces LDL-derived phospholipid hydroperoxides in atherogenic mixed dyslipidemia. J Lipid Res *57*, 2073-2087. 10.1194/jlr.P068585.

34. Pirillo, A., and Catapano, A.L. (2017). Pitavastatin and HDL: Effects on plasma levels and function(s). Atheroscler Suppl *27*, e1-e9. 10.1016/j.atherosclerosissup.2017.05.001.

Supporting information

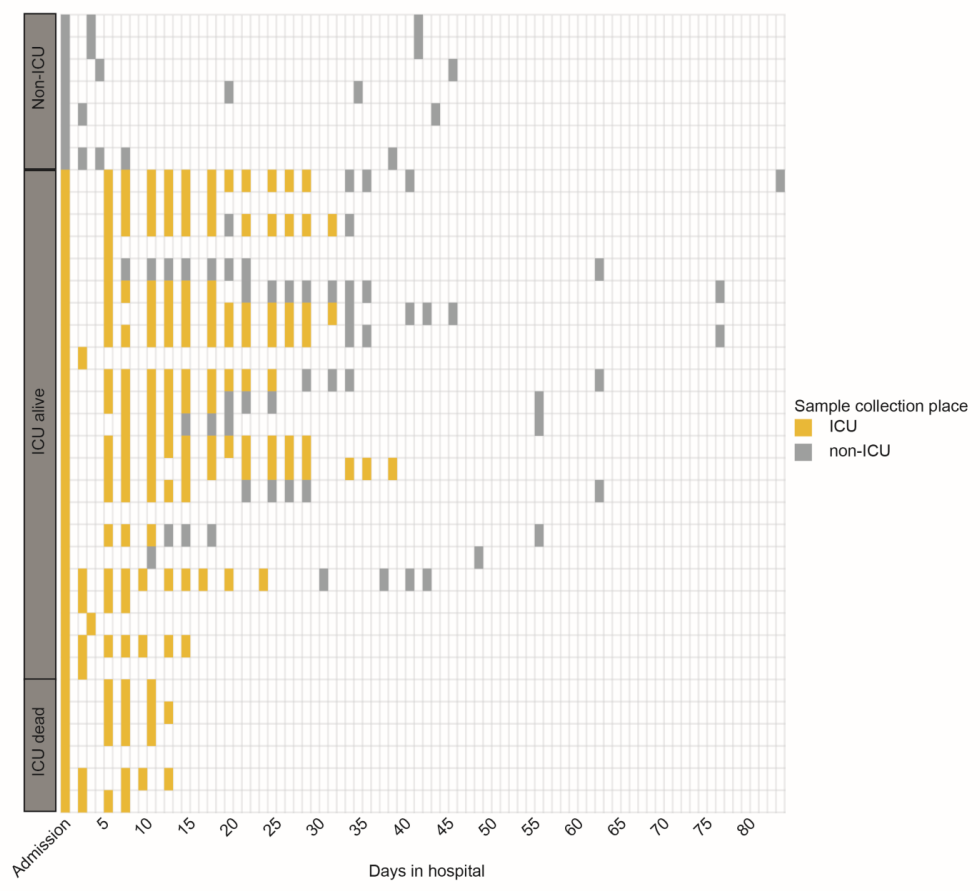

Supplemental figure S1. Timeline of the longitudinal sample collection in the present study.

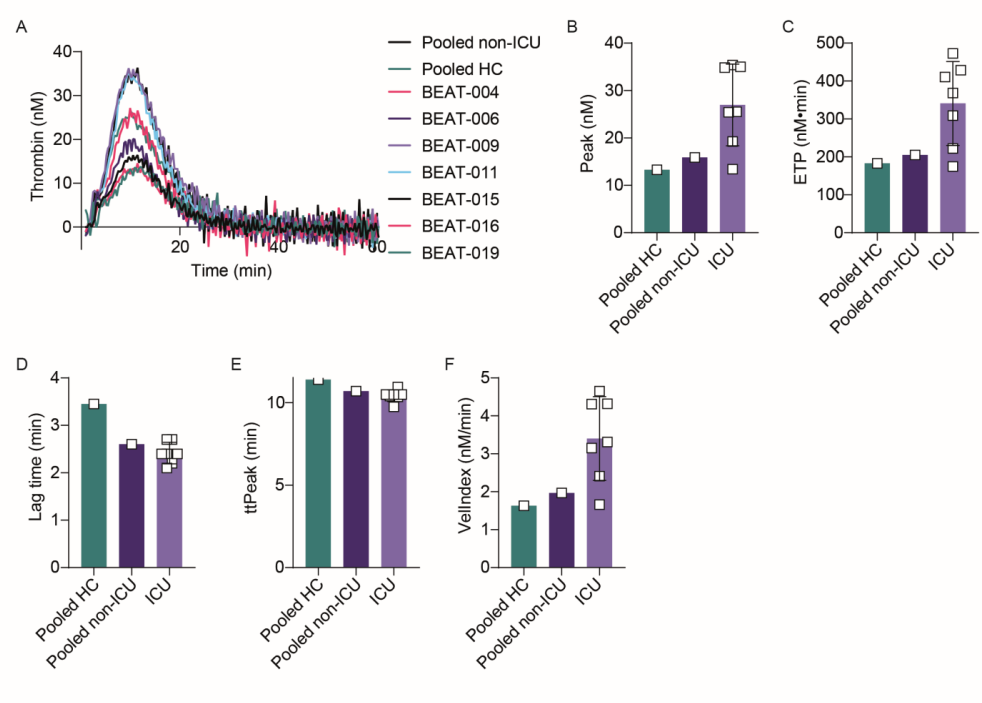

Supplemental figure S2. Impaired HDL anti-thrombotic capacity in COVID-19 patients. (A) Thrombin generation curve of pooled healthy control (n = 1), pooled non-ICU COVID-19 (n = 1), and ICU COVID-19 patients (n = 7). (B) Difference of thrombin peak height between pooled healthy control, pooled non-ICU COVID-19, and ICU COVID-19 patients. (C) Difference of ETP between pooled healthy control, pooled non-ICU COVID-19, and ICU COVID-19 patients. (E) Difference of lag time between pooled healthy control, pooled non-ICU COVID-19, and ICU COVID-19 patients. (F) Difference of time to peak between pooled healthy control, pooled non-ICU COVID-19, and ICU COVID-19 patients. (G) Difference of thrombin generation velocity between pooled healthy control, pooled non-ICU COVID-19, and ICU COVID-19 patients.

Supplemental table S1. Clinical and experimental characteristics of the study population.

	COVID-19 patients (n = 37)	non-ICU (n = 5)	ICU survivors (n = 26)	ICU non-survivors (n = 6)	Healthy controls (n = 12)
Demographic					
Sex (% women)	18.92	20	19.23	16.67	25
Age, y	61 (57-70)	50 (46-61)	65 (59-71)	60 (58-64)	60 (60-60)
Respiratory function					
Respiratory rate	27.24 (7.53)	19.6 (4.56)	27.09 (6.49)	34.17 (7.25)	-
SpO_2	90.36 (2.76)	94.8 (1.64)	90.05 (1.96)	87.83 (1.6)	-
FiO_2	60 (41-100)	-	53 (40-85)	88 (64-100)	-
PaO_2/FiO_2	16.7 (5.27)	-	17.85 (4.78)	13.08 (5.49)	-
Disease severity score					
GCS	3 (3-14)	15 (15-15)	4 (3-11)	3 (3-3)	-
LUMC severity score	12 (9-14)	3 (1-4)	12 (11-13)	16 (13-17)	-
SOFA score	7 (7-11)	-	8 (6-11)	7 (7-10)	-
Circulating markers					
Urea, mg/L	13 (5.15-16.8)	4.75 (4.32-5.05)	14.6 (7.35-17.78)	14.1 (12.85-15.5)	-
CRP, mmol/L	164.35 (61.77-243.7)	102.7 (70.05-139.33)	145 (48.05-239.08)	240.25 (181.45-259.75)	-
Circulating Angiopoietin 2, ng/mL	8.2 (6.21-16.4)	6.3 (4-6.55)	8.36 (5.86-17.09)*	11.2 (8.16-19.49)*	4.45 (2.4-5.53)
Circulating soluble thrombomodulin, ng/mL	14.46 (9.9-19.95)	9.2 (7.75-11.05)	16.51 (11.04-21.58)*	16.06 (9.77-19.69)	6.4 (5.38-8)
Circulating soluble Syndecan 1, ng/mL	9.8 (7.88)	4.3 (3.3)	9.32 (7.35)	14.85 (10.51)	6.26 (5.14)
***In vitro* endothelial functional assay parameters**					
Supernatant Angiopoietin 2, ng/mL	27.39 (10.55)	14.63 (1.62)	29.06 (9.08)*#	32.44 (12.19)*#	13.63 (1.09)
Supernatant Interleukin 6, pg/mL	256.13 (146.4)	71.36 (16.84)	262.44 (121.31)*#	389.08 (130.15)*#	68.11 (13.95)
Supernatant soluble thrombomodulin, ng/mL	2.6 (1.21)	1.19 (0.46)	2.65 (0.88)*#	3.59 (1.59)*#	1.1 (0.21)
Supernatant Von Willebrand factor, U/mL	27.8 (22.9-46.46)	-	30.07 (14.14)*#	49.01 (23.67)*#$	3.51 (2.04)
Xa generation 1hr, nM	0.22 (0.04)	0.15 (0.01)	0.22(0.03)*#	0.25 (0.03)*#	0.14 (0.02)
Xa generation 2hrs, nM	0.23 (0.06)	0.15 (0.02)	0.23 (0.05)*#	0.27 (0.05)*#	0.15 (0.02)
Thrombin peak height, nM	7.51 (2.87-11.5)	0.74 (0.56-1.03)	8.39 (5.1-14.08)*	8.89 (6.76-10.64)*	0.7 (0.59-0.9)
ECIS HPMEC resistance, AUC	17160 (15802-18544)	19085 (19046-19727)	17160 (15589-18321)*	16193 (15366-16766)*#	19252 (18761-19558)
ECIS HPMEC Rb, AUC	131.1 (118-143)	145 (145-154)	134 (116-141)*	120 (115-127)*#	146 (144-149)
ECIS GEnC resistance, AUC	8577.52 (690.87)	9348.6 (197.52)	8497.9 (688.04)*	8200.33 (493.03)*#	9195.42 (547.29)
ECIS GEnC Rb, AUC	44.62 (5.89)	51.78 (2.31)	43.48 (5.87)*#	42.48 (3.33)#	49.65 (3.95)

Data are shown as mean (± SD), median (25th percentile–75th percentile), or percentage. One-way ANOVA followed by Tukey's multiple comparisons test or Kruskal-Wallis followed by Dunn's multiple comparisons test were performed; healthy control as reference: *p<0.05; non-ICU as reference: #p<0.05.

Abbreviations: *CRP* C-reaction protein; *ECIS* Electric cell-substrate impedance sensing system; *FiO_2* Fraction of inspired oxygen; *GCS* Glasgow Coma Scale; *PaO_2* Partial pressure of oxygen; *Rb* Resistance between cells; *SOFA score* Sequential organ failure assessment score; *SpO_2* Oxygen saturation.

Supplemental table S2. Quantified HDL-related lipoprotein subfractions.

Abbreviation	Lipoprotein subfraction
TPA1	Total apolipoprotein A1 (ApoA1)
TPA2	Total apolipoprotein A2 (ApoA2)
HDA1	ApoA1 content in total HDL
HDA2	ApoA2 content in total HDL
HDCH	Cholesterol content in total HDL
HDFC	Free Cholesterol content in total HDL
HDPL	Phospholipid content in total HDL
HDTG	Triglyceride content in total HDL
H1A1	ApoA1 content in HDL-1 subclass
H1A2	ApoA2 content in HDL-1 subclass
H1CH	Cholesterol content in HDL-1 subclass
H1FC	Free Cholesterol content HDL-1 subclass
H1PL	Phospholipid content in HDL-1 subclass
H1TG	Triglyceride content in HDL-1 subclass
H2A1	ApoA1 content in HDL-2 subclass
H2A2	ApoA2 content in HDL-2 subclass
H2CH	Cholesterol content in HDL-2 subclass
H2FC	Free Cholesterol content HDL-2 subclass
H2PL	Phospholipid content in HDL-2 subclass
H2TG	Triglyceride content in HDL-2 subclass
H3A1	ApoA1 content in HDL-3 subclass
H3A2	ApoA2 content in HDL-3 subclass
H3CH	Cholesterol content in HDL-3 subclass
H3FC	Free Cholesterol content HDL-3 subclass
H3PL	Phospholipid content in HDL-3 subclass
H3TG	Triglyceride content in HDL-3 subclass

H4A1	ApoA1 content in HDL-4 subclass
H4A2	ApoA2 content in HDL-4 subclass
H4CH	Cholesterol content in HDL-4 subclass
H4FC	Free Cholesterol content HDL-4 subclass
H4PL	Phospholipid content in HDL-4 subclass
H4TG	Triglyceride content in HDL-4 subclass

Supplemental table S3. Differential HDL composition between non-ICU COVID-19 patients and healthy controls based on multinomial logistic regression analysis. (Reference: healthy controls)

HDL composition	Regression coefficient (β)			P value
	β	CI2.5	CI97.5	
HDCH	-2.42	-3.10	-1.73	4.11E-12
TPA1	-2.29	-2.95	-1.63	1.14E-11
TPA2	-2.96	-3.84	-2.09	3.32E-11
HDTG	1.10	0.53	1.67	1.38E-04
HDFC	-1.33	-1.77	-0.89	2.57E-09
HDPL	-1.42	-1.85	-0.99	1.36E-10
HDA1	-2.41	-3.10	-1.73	5.08E-12
HDA2	-2.41	-3.06	-1.76	3.10E-13
H1TG	0.93	0.39	1.47	7.62E-04
H2TG	2.07	1.25	2.89	7.53E-07
H3TG	1.21	0.67	1.75	1.07E-05
H4TG	0.77	0.35	1.20	3.89E-04
H1CH	-0.53	-0.88	-0.18	2.96E-03
H2CH	-1.34	-1.78	-0.90	1.75E-09
H3CH	-2.85	-3.64	-2.06	1.66E-12
H4CH	-3.93	-5.25	-2.61	6.01E-09
H1FC	-1.03	-1.41	-0.65	1.40E-07
H2FC	-1.60	-2.06	-1.14	7.35E-12
H3FC	-2.00	-2.53	-1.46	2.74E-13
H4FC	-1.56	-2.09	-1.03	8.94E-09
H1PL	-0.48	-0.85	-0.10	1.32E-02
H2PL	-1.04	-1.47	-0.60	3.31E-06
H3PL	-1.58	-2.04	-1.13	8.96E-12
H4PL	-1.71	-2.28	-1.14	4.83E-09
H1A1	-0.51	-0.88	-0.14	7.03E-03
H2A1	-1.78	-2.26	-1.30	3.48E-13
H3A1	-1.87	-2.37	-1.37	2.98E-13
H4A1	-3.23	-4.30	-2.16	2.95E-09
H1A2	-0.69	-1.11	-0.27	1.18E-03
H2A2	-0.78	-1.18	-0.38	1.39E-04
H3A2	-1.29	-1.71	-0.87	1.59E-09
H4A2	-3.16	-4.19	-2.13	2.02E-09

Supplemental table S4. Differential HDL composition between ICU COVID-19 patients and healthy controls based on multinomial logistic regression analysis. (Reference: healthy controls)

HDL composition	Regression coefficient (β)			P value
	β	CI2.5	CI97.5	
HDCH	-2.38	-3.04	-1.73	9.19E-13
TPA1	-2.59	-3.24	-1.94	8.22E-15
TPA2	-3.11	-3.97	-2.25	1.50E-12
HDTG	1.77	1.21	2.33	6.06E-10
HDFC	-1.33	-1.73	-0.93	7.41E-11
HDPL	-0.83	-1.18	-0.48	3.02E-06
HDA1	-2.59	-3.26	-1.92	2.98E-14
HDA2	-2.26	-2.87	-1.66	2.63E-13
H1TG	1.50	0.98	2.03	1.88E-08
H2TG	3.82	2.90	4.74	4.44E-16
H3TG	2.04	1.48	2.59	5.53E-13
H4TG	0.74	0.35	1.14	2.32E-04
H1CH	-0.36	-0.65	-0.07	1.56E-02
H2CH	-0.59	-0.95	-0.23	1.44E-03
H3CH	-2.75	-3.51	-1.99	1.44E-12
H4CH	-5.18	-6.56	-3.81	1.72E-13
H1FC	-0.95	-1.27	-0.62	1.15E-08
H2FC	-0.75	-1.12	-0.39	6.11E-05
H3FC	-1.72	-2.19	-1.25	1.10E-12
H4FC	-2.42	-2.99	-1.85	0.00E+00
H1PL	-0.03	-0.33	0.27	8.46E-01
H2PL	0.34	-0.01	0.68	5.85E-02
H3PL	-0.63	-0.97	-0.30	2.32E-04
H4PL	-2.35	-2.94	-1.77	3.11E-15
H1A1	-0.12	-0.41	0.17	4.12E-01
H2A1	-0.69	-1.04	-0.33	1.52E-04
H3A1	-1.46	-1.89	-1.02	5.58E-11
H4A1	-4.62	-5.76	-3.48	2.00E-15
H1A2	0.13	-0.18	0.44	4.20E-01
H2A2	0.01	-0.31	0.33	9.67E-01
H3A2	-0.68	-1.00	-0.36	3.90E-05
H4A2	-4.16	-5.23	-3.09	3.02E-14

Supplemental table S5. Differential HDL composition between non-ICU COVID-19 patients and ICU COVID-19 patients based on multinomial logistic regression analysis. (Reference: non-ICU COVID-19 patients)

HDL composition	Regression coefficient (β)			P value
	β	CI2.5	CI97.5	
HDCH	0.03	-0.28	0.34	8.35E-01
TPA1	-0.30	-0.63	0.03	7.46E-02
TPA2	-0.15	-0.48	0.18	3.86E-01
HDTG	0.67	0.33	1.00	1.09E-04
HDFC	0.01	-0.29	0.30	9.73E-01
HDPL	0.59	0.27	0.91	2.49E-04
HDA1	-0.18	-0.50	0.14	2.73E-01
HDA2	0.15	-0.18	0.47	3.79E-01
H1TG	0.57	0.26	0.89	3.41E-04
H2TG	1.75	1.19	2.31	8.86E-10
H3TG	0.83	0.47	1.19	6.46E-06
H4TG	-0.03	-0.29	0.23	8.22E-01
H1CH	0.17	-0.11	0.46	2.34E-01
H2CH	0.75	0.45	1.05	1.28E-06
H3CH	0.10	-0.22	0.41	5.45E-01
H4CH	-1.25	-1.66	-0.85	1.13E-09
H1FC	0.08	-0.23	0.39	5.99E-01
H2FC	0.85	0.53	1.17	2.32E-07
H3FC	0.28	-0.05	0.61	9.84E-02
H4FC	-0.86	-1.21	-0.52	9.54E-07
H1PL	0.45	0.14	0.75	4.20E-03
H2PL	1.37	1.00	1.75	1.06E-12
H3PL	0.95	0.60	1.30	1.17E-07
H4PL	-0.64	-0.98	-0.31	1.38E-04
H1A1	0.39	0.08	0.69	1.23E-02
H2A1	1.10	0.73	1.46	3.74E-09
H3A1	0.41	0.10	0.72	9.87E-03
H4A1	-1.39	-1.81	-0.97	1.05E-10
H1A2	0.82	0.47	1.17	4.53E-06
H2A2	0.79	0.46	1.11	2.10E-06
H3A2	0.61	0.29	0.93	2.07E-04
H4A2	-1.00	-1.37	-0.63	1.38E-07